NATURE|Vol 460|13 August 2009|doi:10.1038/nature08303

Mechanistic considerations of halogenating enzymes

Alison Butler[1] & Moriah Sandy[1]

In nature, halogenation is a strategy used to increase the biological activity of secondary metabolites, compounds that are often effective as drugs. However, halides are not particularly reactive unless they are activated, typically by oxidation. The pace of discovery of new enzymes for halogenation is increasing, revealing new metalloenzymes, flavoenzymes, *S*-adenosyl-L-methionine (SAM)-dependent enzymes and others that catalyse halide oxidation using dioxygen, hydrogen peroxide and hydroperoxides, or that promote nucleophilic halide addition reactions.

Halogenated natural products have been isolated in abundance from marine eukaryotic organisms, but also increasingly from microorganisms that inhabit marine and terrestrial environments (Fig. 1). These halogenated compounds range from peptides, polyketides, indoles, terpenes, acetogenins and phenols to volatile halogenated hydrocarbons (for example bromoform, chloroform and dibromomethane) that are produced on a very large scale[1–3]. Many halogenated marine metabolites possess biological activities of pharmacological interest, including anticancer, antifungal, antibacterial, antiviral and anti-inflammatory activities. The biogenesis of these compounds has intrigued scientists for decades.

The first halogenating enzyme to be discovered, in the 1960s, was the haem (iron-containing porphyrin) chloroperoxidase (CPO) from the terrestrial fungus *Caldariomyces fumago*, which produces the chlorinated natural product caldariomycin[4]. Some time later, haloperoxidase enzymes were proposed in the biogenesis of certain halogenated marine natural products[5,6], although this was long before haloperoxidases or other halogenating enzymes had been discovered in marine organisms. Since the discovery of haem CPO, other haem haloperoxidases[7–9], vanadium haloperoxidases[10–12] and non-haem iron halogenases[13], as well as non-metallo-, flavin-dependent halogenases[14], SAM-dependent chlorinases and fluorinases[15], and methyl halide transferases[16], have been discovered. For recent reviews, see refs 14, 15, 17–23.

Haloperoxidases catalyse electrophilic halogenation reactions, whereas the non-haem iron halogenases catalyse radical halogenation reactions and SAM-dependent halogenases catalyse nucleophilic halogenation reactions. Haloperoxidases have traditionally been classified on the basis of the most electrophilic halide that is readily oxidized. Thus, chloroperoxidases oxidize chloride, bromide and iodide by hydrogen peroxide (H_2O_2), whereas iodoperoxidases oxidize only iodide in this way. Hydrogen peroxide lacks the thermodynamic potential to oxidize fluoride; thus, enzymes catalysing fluorination are not peroxidases. The overall stoichiometry of the haloperoxidase reaction is consumption of one equivalent of H_2O_2 per halogenated product produced (Fig. 2, reaction 1).

One class of halogenase, the non-haem iron enzymes, uses dioxygen (O_2) to activate halide (Fig. 2, reaction 2); these enzymes catalyse radical halogenation reactions at aliphatic carbon sites. The overall stoichiometry is consumption of one equivalent of α-ketoglutaric acid and O_2 per halogenated equivalent produced (Fig. 2, reaction 2). Flavin-dependent halogenases activate O_2 by means of formation of flavin-bound hydroperoxide, which then oxidizes the halide (Fig. 2, reaction 3). This class of halogenating enzyme is a two-component system in which a flavin reductase is required to keep the halogenase reduced for catalytic turnover. These enzymes catalyse reactions that more closely resemble the electrophilic haloperoxidases that are mediated by 'HOX-like' species. Finally, SAM-dependent enzymes catalyse nucleophilic substitution, generating 5′-halo-5′-deoxyadenosine and L-methionine (Fig. 2, reaction 4). In this review we focus on the mechanisms of metalloenzyme-catalysed halogenation reactions, emphasizing the activation of halides by O_2 and H_2O_2, and the nature of the halogenation step.

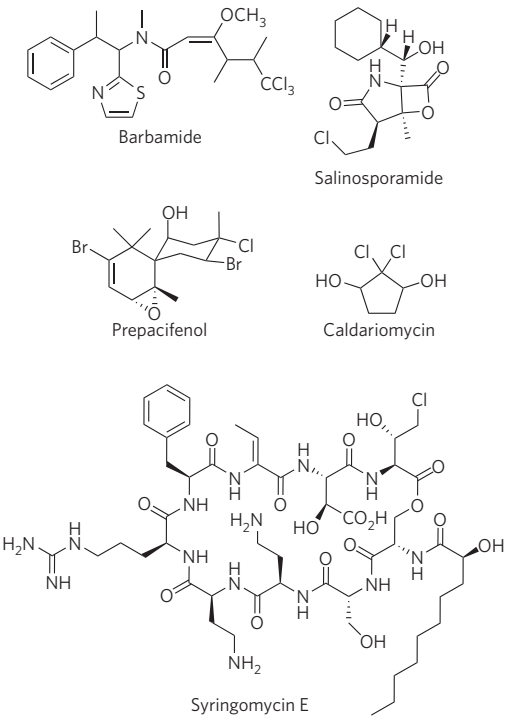

Figure 1 | Halogenated natural products. A few examples of halogenated natural products that have been discovered in the past few decades. These natural products have been isolated from marine eukaryotic organisms, as well as microorganisms that inhabit marine and terrestrial environments.

[1]Department of Chemistry and Biochemistry, University of California, Santa Barbara, California 93106, USA.

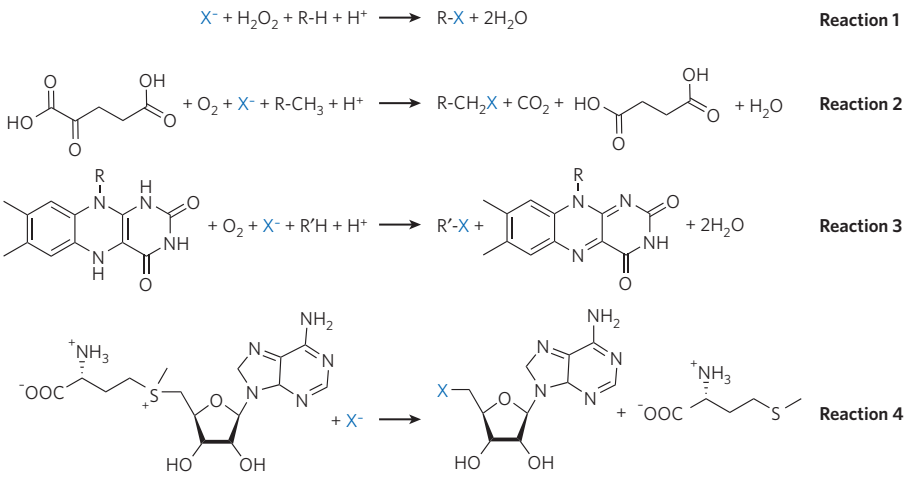

Figure 2 | Biologically relevant halogenation reactions. Four distinct classes of enzyme have been discovered that carry out halogenation reactions. Reaction 1, which encompasses electrophilic halogenation, is catalysed by haloperoxidases such as the haem-containing or vanadate-containing enzymes. Reaction 2 is carried out by α-ketoglutarate-dependent non-haem iron halogenases and is characteristic of radical halogenation at unactivated C–H centres. Reaction 3 is catalysed by flavin-dependent halogenases. Reaction 4 shows the SAM-dependent halogenase reaction. X, halogen atom; R, R′, alkyl group.

Haem haloperoxidases

The fungus *C. fumago*, from which the first haloperoxidase, Fe(III)-haem CPO, was derived[4], produces the chlorinated natural product caldariomycin, which is thought to be synthesized by CPO. The optimal pH for chlorination turnover by haem CPO is pH 2.7 (ref. 4). Interestingly, CPO is used to catalyse a number of oxidation reactions in the absence of chloride. These oxidation reactions are generally carried out at neutral pH, whereas chlorination occurs only at low pH. The active site of Fe(III)-haem CPO contains Fe(III)-protoporphyrin IX coordinated by the thiolate side chain of a cysteine in the proximal position[24]. Recently the X-ray structure of Fe(III)-haem CPO was determined with the substrate, 1,3-cyclopentanedione (CPD), bound in one of the two channels leading to the haem iron centre (Fig. 3)[25]. In addition, halide-binding sites were identified at the protein surface near the opening of the second, narrower, channel leading to the haem iron moiety, as well as within this channel and at the other end of the channel, near the haem iron site[25].

A haem bromoperoxidase isolated from the marine green alga *Penicillus capitatus* contains a distal His ligand in place of the cysteine ligand in Fe(III)-haem CPO[7,8]. This enzyme uses bromide preferentially, although under certain conditions it can catalyse chlorination reactions[8]. Although the thiolate ligand was initially thought to be important for CPO activity, and His for bromoperoxidase activity in the haem haloperoxidases, a haem CPO with a distal His ligand has been isolated from the marine worm *Notomastus lobatus*[9]. This enzyme is unusual in that it requires a partner flavoprotein for activity.

The haem iron centre functions as a redox catalyst (Fig. 4). Hydrogen peroxide oxidizes the haem Fe(III) centre to compound I, the Fe(IV)-oxo π-cation radical species (O=Fe(IV)-haem$^{+\bullet}$), via the short-lived compound-0 state, characterized as a peroxo-anion complex, HOO–Fe(III)-haem[26]. Glu 183 is proposed to assist in formation of both compound 0 and compound I. Compound I oxidizes chloride by two electrons, reforming the haem Fe(III) centre. Characterization of the state that is generated immediately following chloride oxidation has generated much discussion[27]. At issue is whether OCl^- is a ligand to the Fe(III)-haem at the distal site, whether it is released from the enzyme active site or whether it is otherwise trapped within the enzyme substrate pocket but not coordinated to Fe(III)-haem. The oxidized chlorine intermediate can then chlorinate the organic substrate or react with a second equivalent of H_2O_2, producing O_2 (in the singlet excited state). Although caldariomycin (Fig. 1) is not a chiral compound, interest in stereospecific and regiospecific halogenation reactions has been widespread.

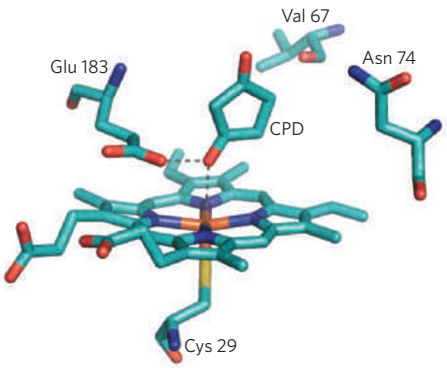

Figure 3 | Structure of the active site of haem CPO from *C. fumago*, with a bound substrate, 1,3-cyclopentanedione[25]. The active site of CPO contains Fe(III)-protoporphyrin IX coordinated by the thiolate side chain of a Cys in the proximal position. Two channels have been identified that lead to the haem active site. The substrate, 1,3-cyclopentanedione (CPD), has been located in the broader of the two channels in a recent X-ray structure, and halides were located within the narrower channel[25]. Glu 183 is located close to the haem iron centre and is proposed to assist in formation of both compound 0 and compound I (Fig. 4). The carbon backbone is shown in teal green, oxygen in red, nitrogen in blue, sulphur in yellow and the Fe(III) centre in orange; the dashed lines indicate hydrogen bonding.

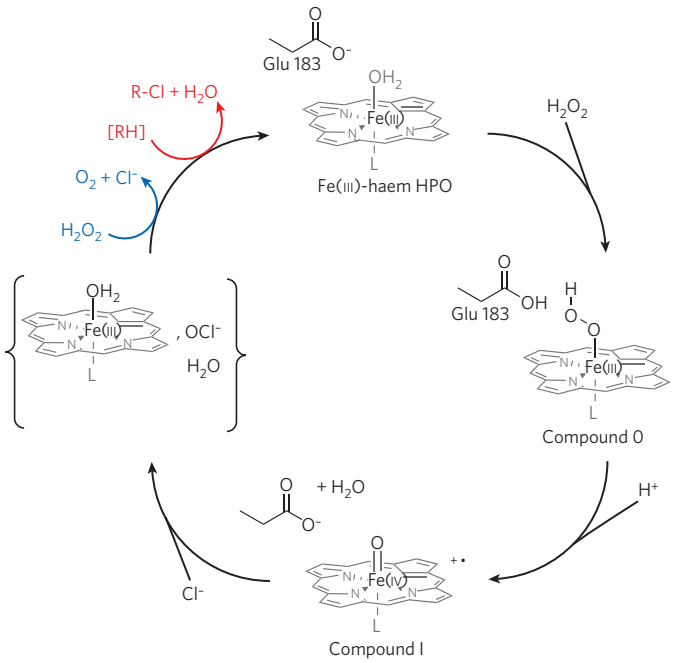

Figure 4 | Proposed catalytic cycle for haem CPOs[24–27]. The Fe(III)-haem resting state is oxidized by H_2O_2, forming compound I. Compound I oxidizes chloride by two electrons, reforming the haem Fe(III) centre and generating an oxidized chlorine intermediate that is formally at the oxidation level of OCl^-. This oxidized chlorine intermediate could chlorinate the organic substrate (shown in red) or oxidize a second equivalent of H_2O_2 (shown in blue), depending on the reaction conditions. L, cysteine.

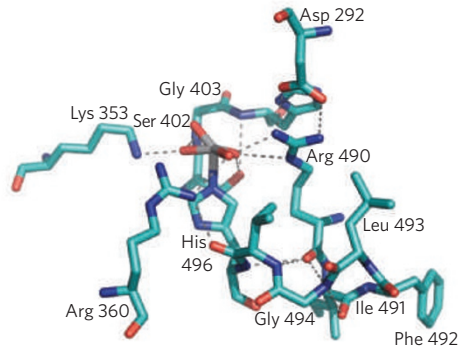

Figure 5 | Structure of the active site of V-CPO from *C. inaequalis*[35]. The V(v)-containing active site shown here for V-CPO is very similar in all the V-HPOs. A conserved His residue is a ligand to vanadate. The carbon backbone is shown in teal green, oxygen in red, nitrogen in blue and the V(v) centre in grey; the dashed lines indicate hydrogen bonding.

Numerous kinetic and spectroscopic investigations along with product analyses have tried to probe the nature of the halogenating intermediate. Several experimental results suggest that the oxidized chlorine intermediate may not escape from the active site during turnover[27]. A key result arising from Cl^- oxidization by compound I, which is the rate-limiting step during turnover, is the $^{35}Cl/^{37}Cl$ isotope effect. During chlorination of 1,3,5-trimethoxybenzene or 3,5-dimethylphenol in the presence of excess chloride (with a known chlorine isotopic composition, $-0.76 \pm 0.07‰$), ^{35}Cl is preferentially incorporated into the chlorinated organic products. The kinetic isotope effect, k_{35}/k_{37} (the ratio of isotope reaction rate constants), of 1.012 for 1,3,5-trimethoxybenzene or 1.011 for 3,5-dimethylphenol is significantly more than that observed in the uncatalysed, molecular chlorination reaction with hypochlorite under otherwise identical conditions[28]. The observed chloride isotope fractionation establishes that the oxidized chlorine intermediate is not in exchange equilibration with bulk Cl^-, Cl_2, OCl^-, HOCl or other possible chlorine species outside the enzyme active site. Thus, this experiment suggests that the oxidized chlorine intermediate is trapped in the enzyme active-site pocket and that chlorination occurs within the enzyme active-site channel.

Vanadium haloperoxidases

The first vanadium haloperoxidase (V-HPO) was discovered in marine kelp in the early 1980s[10,11]. Since that time, vanadium bromoperoxidases (V-BPOs) have been isolated from the three major classes of marine seaweed, and vanadium CPOs (V-CPOs) have been isolated from fungi[29] and are predicted to be present in marine bacteria[30]. V-HPOs are undoubtedly important in the biosynthesis of many halogenated marine natural products (see below), and have recently been shown to be involved in iodide accumulation in marine macroalgae (kelp)[31]. Although chlorinated natural products have not been isolated from the fungi containing V-CPO, these enzymes may be important in fungus-mediated chlorination and degradation of lignin[32].

The vanadate site in V-HPOs is positioned at the bottom of a channel 15–20 Å deep, at the core of the four-helix bundle scaffold (Fig. 5)[33–35]. Vanadium is coordinated to the protein by a single axial His ligand in a trigonal bipyramidal coordination geometry. The three equatorial oxygens of vanadate are hydrogen-bonded to two conserved Arg residues, a Lys, a Ser and the backbone of a Gly amide, thereby decreasing the overall negative charge around the vanadate ion. The proposed apical water/hydroxide ligand is hydrogen-bonded to a His. The X-ray structures of V-BPO (*Corallina officinalis*[34], *Ascophyllum nodosum*[33]) and V-CPO (*Curvularia inaequalis*[35]) are remarkably similar, and are nearly superimposable when the structures are overlaid at the V(v) centre[33]. The striking similarity of the active sites raises questions about the molecular basis of the halide selectivity and the reactivity towards halide oxidation. One noticeable difference in the overlay is the presence of Phe 397 in V-CPO but His in V-BPO. This extra His residue does not interact directly with vanadate, although it has been proposed that the His side chain participates as a proton donor and acceptor during catalysis[23,36,37] and, thus, could affect the overall oxidation potential of the oxo-peroxo-V(v) moiety.

In contrast to the haem haloperoxidases that function as redox catalysts, V-HPOs function as Lewis acid catalysts of halide oxidation by H_2O_2. The catalytic reaction is initiated by coordination of one equivalent of H_2O_2 to the resting V(v) state of the enzyme (Fig. 6a). The X-ray structure of the peroxo adduct of V-CPO reveals that a Lys side chain is hydrogen-bonded to the coordinated peroxide. This is probably an essential feature of the catalytic reaction because it would increase the potential of the oxo-peroxo-V(v) centre for halide oxidation. The oxo-peroxo-V(v) species can then oxidize the halide by two electrons, forming an oxidized halogen that is formally at the X^+ oxidation state or, more probably, at that of the hypohalite anion, OX^-. Electrophilic halogenation results from reaction of 'OX^-' either with the organic substrate or, in the absence of a good organic substrate, with a second equivalent of H_2O_2, forming O_2 (which has been shown to be in the singlet excited state during turnover with Br^-)[38] and the halide, X^-. Radical halogenation reactions have not been observed with the V-HPO enzymes.

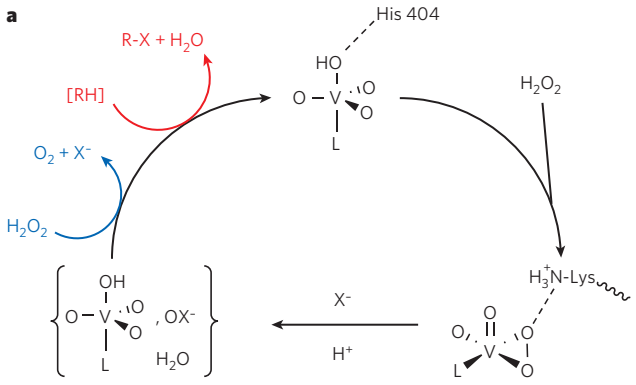

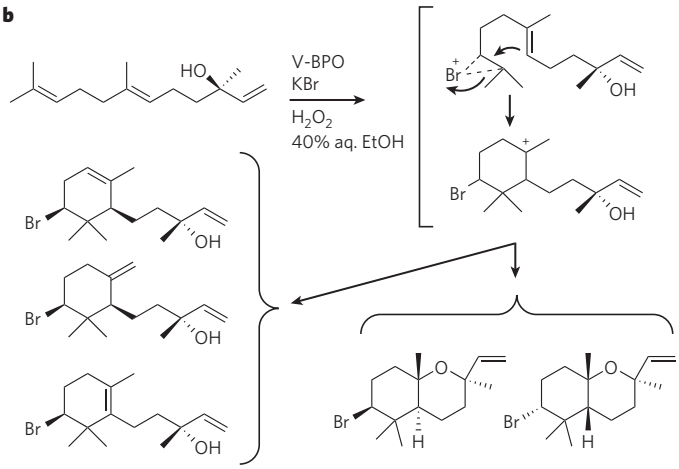

Figure 6 | Mechanistic considerations of V-HPOs. **a**, Proposed catalytic cycle for V-HPOs[12,21,23,37]. The catalytic reaction is initiated by coordination of one equivalent of H_2O_2 to the resting V(v) state of the enzyme. Hydrogen bonding from a Lys side chain to V(v)-coordinated peroxide most probably assists halide oxidation by increasing the oxidation potential of the oxo-peroxo-V(v) moiety. After halide oxidation, the oxidized halogen intermediate, 'OX^-', could brominate the organic substrate (shown in red) or oxidize a second equivalent of H_2O_2, forming singlet oxygen (shown in blue). **b**, V-BPO-catalysed formation of α-, β- and γ-snyderol and (+)-3β-bromo-8-epicaparrapi oxide natural products from (*E*)-(+)-nerolidol[41]. The formation of single diastereomers of α-, β- and γ-snyderol suggests that the reaction proceeds through a common intermediate, initially formed by electrophilic bromination of a single face of the terminal alkene site in (*E*)-(+)-nerolidol. L, ligand.

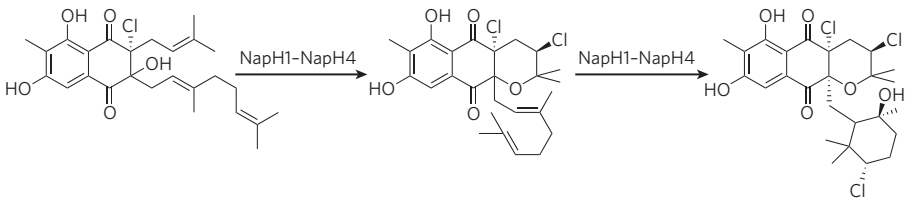

Figure 7 | Proposed biosynthesis of the napyradiomycins A80915A–A80915D[30]. The sequence of reactions depicts chlorination and cyclization of the isoprene and the geranyl units in a manner analogous to V-BPO-catalysed bromination and cyclization of terpenes shown in Fig. 6b.

Initial reports suggested that V-BPO lacked organic-substrate specificity because a wide range of brominated organic compounds could be produced. However, few compounds are brominated as efficiently as would be indicated by the stoichiometric consumption of one equivalent of H_2O_2 per brominated organic equivalent produced (Fig. 2, reaction 1). Instead, during halogenation reactions of many compounds, far more H_2O_2 is consumed in the halide-assisted H_2O_2-disproportionation reaction than brominated product is formed, consistent with escape of HOBr from the active site as occurs with poor organic substrates.

Terpenes, which are the biogenic precursors to many halogenated terpene natural products, are substrates for V-BPO that do react stoichiometrically during turnover, such that one equivalent of H_2O_2 is consumed per equivalent of terpene reacted, at least with the red algal V-BPOs[39–41]. For example, V-BPO catalyses the bromination of the sesquiterpene (*E*)-(+)-nerolidol, which is accompanied by terpene cyclization, and consumption of one equivalent of H_2O_2 in the formation of α-, β- and γ-snyderol and (+)-3β-bromo-8-epicaparrapi oxide (Fig. 6b)[41]. Single diastereomers of β- and γ-snyderol and mixed diastereomers of (+)-3β-bromo-8-epicaparrapi oxide (diastereomeric excess, 20–25%) are produced in the V-BPO-catalysed reaction with (*E*)-(+)-nerolidol, whereas two diastereomers of these compounds are formed in the synthesis with 2,4,4,6-tetrabromocyclohexa-2,5-dienone[41].

The formation of single diastereomers of the snyderols in the V-BPO reaction indicates that only one face of the terminal alkene of (*E*)-(+)-nerolidol is brominated. Moreover, the halogenating species is trapped within the active site, although speciation within the active site, such as $HOBr/OBr^-/Br_2$, V(v)-OBr or a possible bromamine or acyl hypobromite species, among other possibilities, cannot be addressed explicitly. Thus, the active-site channel would seem to play a role by holding the terpene substrate in place such that only one face of the terminal alkene is presented to the vanadium centre. Differences between the active-site channels, in terms of terpene-substrate selectivity, is a topic of current interest.

Recent cluster analysis of the napyradiomycin biosynthetic gene cluster (*nap*) from the marine sediment *Streptomyces* sp. strain CNQ-525 and the actinomycete *Streptomyces aculeolatus* NRRL 18442 revealed multiple open-reading-frame sequences that could encode multiple V-CPOs and a flavin-dependent halogenase. Functional expression of the biosynthetic cluster leads to formation of chlorinated compounds (Fig. 7); however, a functional V-CPO has not yet been isolated[30].

Phylogenetic analysis of V-HPOs shows that the *nap* V-CPOs form a clade distinct from the marine algal V-BPO clade (*A. nodosum*, *Corallina pilulifera* and *C. officinalis*) and the fungal V-CPO clade (*C. inaequalis* and *Embellisia didymospora*)[30]. All of the V-HPOs have a set of conserved residues that comprise the His ligand to vanadate (His 496 in the number sequence of *C. inaequalis* V-CPO) and five of the other amino acids at the active site, most of which are involved in hydrogen-bonding to vanadate oxygen atoms. However, His 404, a residue that is found within hydrogen-bonding distance of the vanadate apical oxygen, is absent in the putative *nap* V-CPOs[30]. It will be interesting to learn the effects that the His 404 substitutions (Ser, Phe) have on halide oxidation reactivity.

In an interesting display of chemical defence, some marine algae have evolved a means to disrupt bacterial quorum sensing and, thus, mitigate the effects of bacterial colonization of an alga's surface. Quorum sensing is the mechanism by which bacteria sense cell density and regulate such phenotypic responses as biofilm formation, virulence, swarming motility and bioluminescence. Many bacteria use acyl homoserine lactones as their signalling molecules to activate a receptor-mediated cascade of events dependent on sufficient cell density[42].

The lack of microbial fouling of the marine red alga *Delisea pulchra* has intrigued marine ecologists for some time[43]. *Delisea pulchra* produces halogenated furanones that have been shown to inhibit quorum sensing by interfering with the receptor-mediated phenotypic responses of certain bacteria[43]. Intriguingly, the 3-oxo-acyl homoserine lactones are readily susceptible to electrophilic halogenation at C2, as demonstrated by reaction with aqueous $HOX/OX^-/X_2$ as well as by the V-HPO of *Laminaria digitata* (Fig. 8)[44]. The brominated products disrupt quorum sensing efficiently, as demonstrated with engineered reporter strains of *Agrobacterium tumefaciens* and *Chromobacterium violacium*[44]. Some marine algae have haloperoxidases on their surfaces, suggesting that they use a double-pronged approach of attacking 3-oxo-acyl homoserine lactones secreted by bacteria attempting to colonize their surface, in addition to producing halogenated compounds to disrupt quorum sensing.

Non-haem iron halogenases

A number of halogenated natural products, such as syringomycin E, barbamide and jamaicamide, contain halogen substituents at an unactivated carbon centre[13,18,20,22]. The biosynthesis of these compounds is catalysed by a new class of α-ketoglutarate (αKG)-dependent, non-haem iron (Fe_{NH}) halogenase enzymes that comprise a divergent subset of the larger class of Fe_{NH}–αKG oxygenases. In the oxygenase family of enzymes, the bidentate complex of αKG coordinated to Fe(II) is bound in the enzyme active site by coordination to a conserved set of two His ligands and either an Asp or a Glu ligand that form a facial triad at the octahedral iron site. The pentadentate ligation leaves a vacant coordination site for O_2 coordination. Dioxygen activation is coupled to the oxidative decarboxylation of αKG, a co-substrate in the overall enzyme reaction and a source of two of the four electrons required to reduce O_2 to H_2O (Fig. 2, reaction 2).

A distinguishing characteristic of the Fe_{NH}–αKG halogenases is the absence of the carboxylate protein ligand (that is, Glu or Asp). As shown in the X-ray structure of SyrB2, which was the first Fe_{NH} halogenase to be discovered (Fig. 9)[45], Fe(II) is coordinated by the two conserved His ligands and a halide ligand. The conserved Glu/Asp residue has been replaced with Ala; this means that the $(His)_2$(Asp/Glu) triad of the oxygenases has been changed to $(His)_2$(Ala), thus creating a vacancy for the halide.

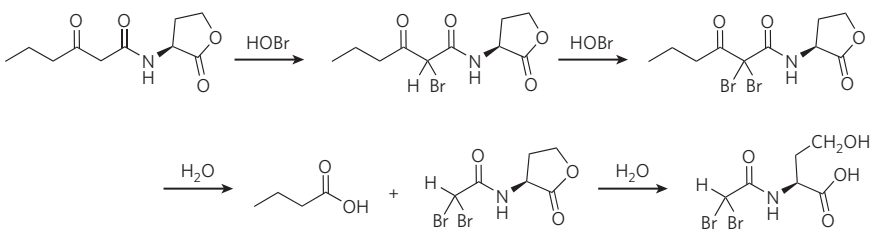

Figure 8 | Bromination of 3-oxo-hexanoyl homoserine lactone and subsequent hydrolysis of the dibromo product[60]. Many bacteria secrete acyl homoserine lactone compounds, which they use as signalling molecules to sense cell density. The 3-oxo class of acyl homoserine lactone is readily susceptible to electrophilic halogenation at C2 with aqueous bromine solutions containing HOBr and Br_2, as shown in this sequence of reactions.

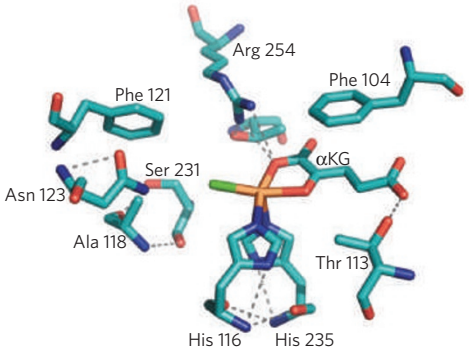

Figure 9 | Structure of the active site of Fe_{NH}–αKG in SyrB2 from *P. syringae*[45]. The active site comprises Fe(II) coordinated to two conserved His ligands and a halide ligand. A conserved Glu/Asp residue found in Fe_{NH}–αKG oxygenases has been replaced by Ala, creating a vacancy for the halide coordination. The carbon backbone is shown in teal green, oxygen in red, nitrogen in blue and the chloride ligand to the non-haem Fe(II) centre (orange) in bright green; the dashed lines indicate hydrogen bonding.

The catalytic cycle of the halogenases (Fig. 10) resembles the reaction sequence of the Fe_{NH}–αKG oxygenases up to the point of formation of the oxo-ferryl species[46,47]. The halogenation reaction begins with association of the organic substrate in the enzyme active site, which triggers a change in the resting state enabling the subsequent coordination of O_2 by Fe(II) in $(His)_2(X^-)Fe(II)_{NH}$–αKG (Fig. 10)[47]. On the basis of the 'HAG' mechanism of the Fe_{NH}–αKG oxygenases[46], Matthews *et al.*[47] have proposed a series of states (I, II and III; Fig. 10) that lead to hydrogen-atom abstraction by the haloferryl (X–Fe(IV)=O) species. The oxygenase and halogenase mechanisms diverge at this point. The halogenase mechanism proceeds by a rebound attack by the halogen atom at the iron centre (Fe(III)–X) on the organic radical leading to the halogenated organic compound and Fe(II), as opposed to rebound by the hydroxyl radical (Fe(III)–OH) in the oxygenase mechanism. The hydrogen-atom abstraction step shows a large deuterium kinetic isotope effect, which has also been observed with other αKG-dependent hydroxylases[47].

The 'substrate triggering' mechanism in the Fe_{NH}–αKG halogenases (Fig. 10) proposed by Matthews *et al.*[47] is consistent with the biosynthesis of syringomycin E (Fig. 1), in which L-threonine is chlorinated by the Fe_{NH}–αKG halogenase component, SyrB2, of the non-ribosomal peptide synthetase biosynthetic gene cluster in *Pseudomonas syringae* B301D (Fig. 11)[48]. A number of other Fe_{NH} halogenases have also been identified or predicted[22], including BarB1 and BarB2 from *Lyngbya majuscula*, which are involved in the trichlorination of L-leucine of barbamide[49]; CytC3 enzymes involved in the sequential chlorination of L-aminobutyrate[50]; and even CmaB, which chlorinates the γ position of L-*allo*-isoleucine (Fig. 11), among others[22,51]. In this last reaction, γ-Cl-L-*allo*-isoleucine undergoes a γ-elimination reaction catalysed by the enzyme CmaC, leading to cyclopropyl ring formation and the release of chloride, a process that has been termed cryptic chlorination[51].

PCR cloning of halogenase homologues has been useful in the discovery of new Fe_{NH}–αKG halogenases[52]. Of particular interest are the Fe_{NH}–αKG halogenase components, CurA and JamE, of *L. majuscula*, which were predicted to be involved in the biosyntheses of curacin A through cryptic halogenation[52] and jamaicamide A through vinyl chloride formation[53]. Very recently, Gu *et al.*[54] demonstrated the remarkable sequence identity of CurA and JamE, at 92%, yet curacin A and jamaicamide A are structurally very different. In the Cur pathway a β-branched cyclopropane is formed, whereas in the Jam pathway a vinyl chloride is formed. The evolution of these metabolic pathways within the same organism is striking. Chlorination occurs at a carboxylated γ-carbon in both pathways, a reaction not previously observed in other halogenases. As depicted in Fig. 12, the biosynthetic pathways diverge after chlorination at the decarboxylation step. After formation of α,β-enoyl thioester (I → II in Fig. 12) in the Cur pathway, the NADPH-dependent Cur enoyl reductase domain was found to catalyse formation of the cyclopropyl unit, presumably by intramolecular nucleophilic displacement of Cl^-. This reaction is new and distinct from the cryptic chlorination reaction catalysed by CmaB (Fig. 11d). However, in the Jam pathway a β,γ-enoyl thioester of the 3-methyl-4-chloroglutaconyl decarboxylation product is formed (I → III in Fig. 12) that is not a substrate for the Jam enoyl reductase. The Jam enoyl reductase domain is a reductase for the α,β-enoyl thioester solely, and thus is not functional in the biosynthesis of jamaicamide.

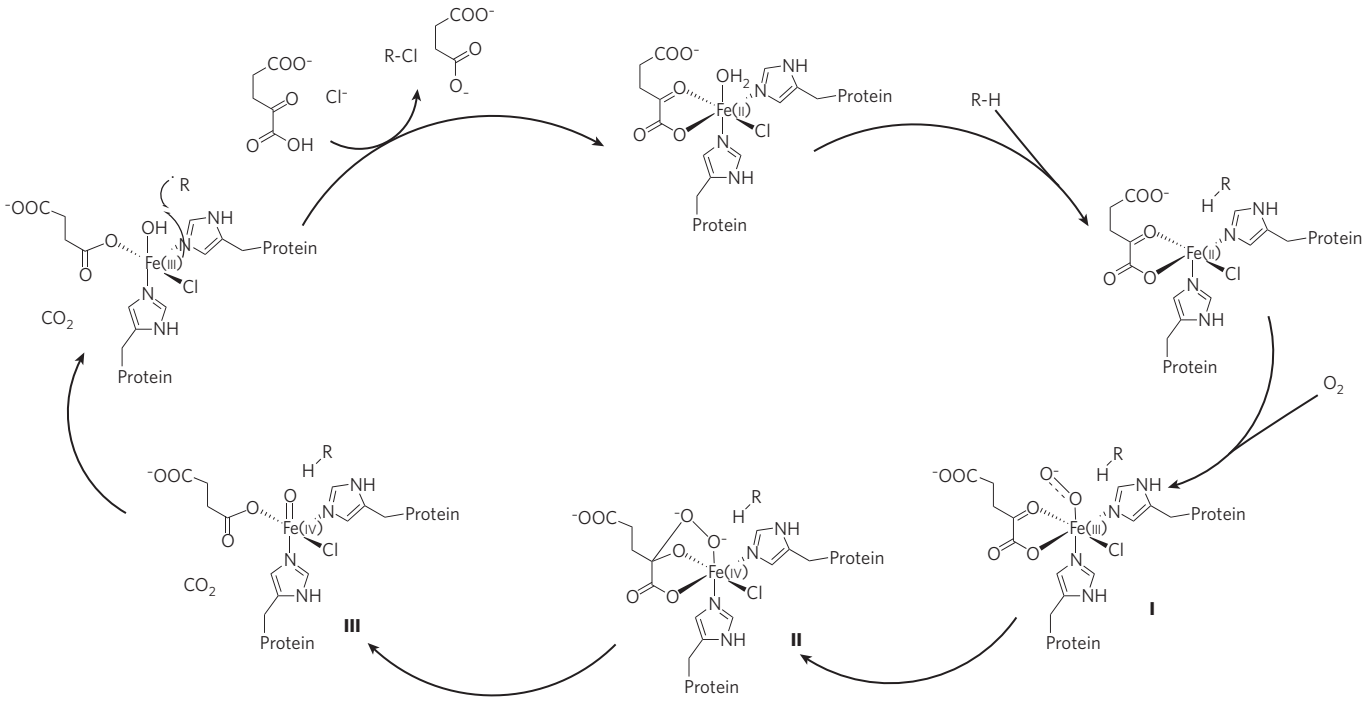

Figure 10 | Proposed catalytic cycle of Fe_{NH}–αKG halogenases. The reaction is triggered on binding of the organic substrate, inducing a conformational change such that the resting $Fe(II)_{NH}$–αKG state can then react with O_2. The scheme shows a series of states — I, II, and III — that lead to hydrogen-atom abstraction by the haloferryl (X–Fe(IV)=O) species. The halogenation reaction can then proceed as described in the main text. Adapted from ref. 47.

Non-metallo-haloperoxidases

Not all biological halogenation is catalysed by metalloenzymes. A large class consists of the flavin-dependent halogenases (Fig. 2, reaction 2; for a current review, see ref. 18). These enzymes carry out halogenation reactions, such as in the biosynthesis of rebeccamycin. Halogenation by perhydrolase enzymes has also been demonstrated, although the biological relevance of this enzyme activity is not known[15].

A significant class of non-metallo-halogenating enzymes use SAM as a co-substrate. The first of the SAM-dependent halogenases to be discovered was the methyl chloride transferase enzyme in seaweeds and other plants, which is responsible for the production of profuse levels of methyl chloride[17,55], raising questions about its biological function. Other SAM-dependent halogenases, including chlorinase[56] and fluorinase[15,56–59] enzymes, are now known. These enzymes catalyse nucleophilic halogenation reactions, rather than electrophilic or radical halogenation reactions. The SAM-dependent chlorinase SalL, from the marine bacterium *Salinospora tropica*, chlorinates SAM by nucleophilic chloride addition generating 5′-chloro-5′-deoxyadenosine as a precursor to chloroethylmalonyl-CoA, which is ultimately incorporated into salinosporamide A[57]. SalL will also accept Br^- and I^- but not F^- directly. The fluorinase is the first step in the biosynthesis of fluoroacetate and 4-fluorothreonine from the soil bacterium *Streptomyces cattleya* at the C5′ site of SAM in a S_N2 reaction that occurs with inversion of configuration[59]

Outlook

In the past five years, more halogenating enzymes have been identified than in the four decades after the discovery of the first halogenating enzyme, haem CPO (*C. fumago*). The pace of discovery of new haloperoxidases and halogenases is bound to continue to increase with the use of genomic and bioinformatic approaches. We will undoubtedly continue to isolate new halogenated natural products and uncover new biosynthetic pathways that co-opt halogenating enzymes for new purposes.

However, in the four-and-a-half decades since the discovery of haem CPO, fundamental questions remain about the mechanism of the halogenating enzymes. At first glance, the intricate balance between halogenation and hydroxylation in the Fe_{NH}–αKG enzymes would seem to be mediated by the replacement of a carboxylic-acid-containing amino acid, Glu or Asp (with Ala in the halogenases), creating a vacant coordination site for halide coordination to iron. But relatively few structures are known for the Fe_{NH}–αKG halogenases. It is not yet known how the Fe_{NH}–αKG active sites vary in this class of enzyme or what the elements of discrimination and selectivity are that exist within these enzyme active sites. The 45-year-old question regarding the nature of the halogenating moiety in the haloperoxidases remains unanswered.

New spectroscopic techniques able to provide faster snapshots during turnover may be revealing. With significant advances in the sensitivity of isotope mass spectrometers, investigations of halogen isotope effects may have a more prominent role in mechanistic investigations, particularly now for $^{79}Br/^{81}Br$ fractionation. Within the V-HPOs, elucidating the factors that control halide selection and positioning, as well as the organic substrate selectivity, will be particularly interesting. The structures of the V-HPOs are fully superimposable at the V(v) centre, yet we know relatively little about the role that the active-site channel has in organic-substrate selectivity, and why some halogenated products predominate in one alga but not another related alga with a very similar haloperoxidase. In consideration of cryptic halogenation, it is not known what other natural products are formed via halogenated intermediates, including possibly in polymerization reactions.

The parallel between haem, non-haem iron and flavin-dependent halogenase enzymes and haem, non-haem iron and flavin-dependent oxygenase enzymes is striking. In addition to these three types of oxygenase enzyme, other oxygenases are also well known, including copper and manganese enzymes. Other metalloenzymes may be involved in halogenation reactions. In retrospect, it is not surprising that marine organisms evolved V-HPOs, given the halide content of the oceans and the fact that vanadium is the second most abundant transition-metal ion in seawater. Organisms living in other salty environments with unique transition-metal-ion compositions also may have evolved new metalloenzymes that carry out halogenation reactions. ■

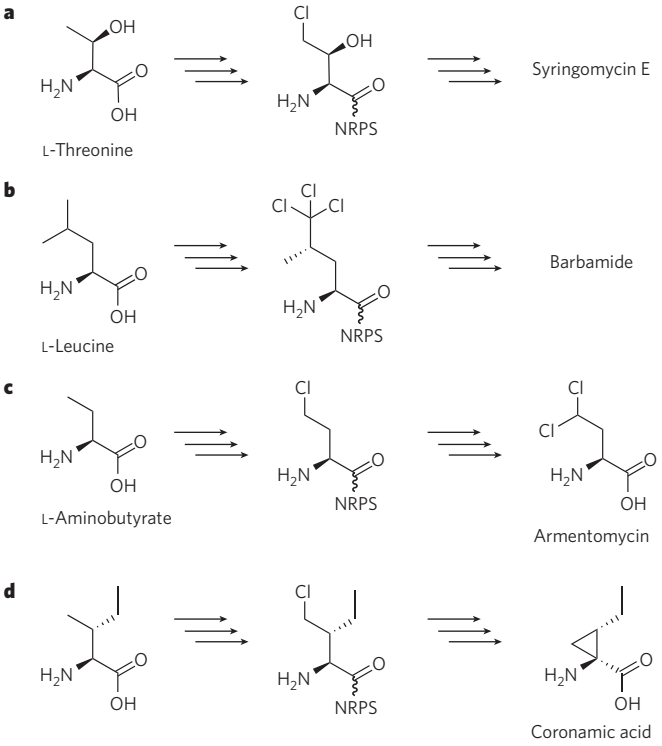

Figure 11 | Examples of Fe_{NH}–αKG halogenase reactions. Fe_{NH}–αKG halogenases have been identified in the biosynthesis of a number of natural products, such as syringomycin E (**a**; Fig. 1), barbamide (**b**; Fig. 1), armentomycin (**c**) and coronamic acid (**d**). The triple arrows mean that multiple reaction steps and different enzymes are required for the indicated conversions. NRPS, non-ribosomal peptide synthetase.

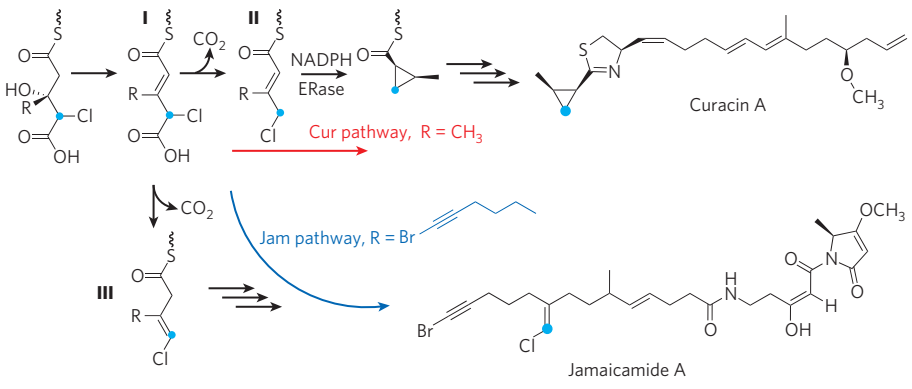

Figure 12 | Parallel assemblies in the biosynthesis of curacin A and jamaicamide A. The pathways diverge after chlorination. ERase, enoyl reductase. The blue dot shows the β-branching carbon atom. Adapted from ref. 54. In the Cur pathway, compound I is converted to an α-β-enoyl thioester (II), which is a substrate for the Cur ERase. In the Jam pathway, compound I is converted to a β-γ-enoyl thioester (III), which is not a substrate for the Jam ERase.

1. Faulkner, D. J. Marine natural products. *Nat. Prod. Rep.* **19,** 1–48 (2002).
2. Gribble, G. W. Naturally occurring organohalogen compounds. *Acc. Chem. Res.* **31,** 141–152 (1998).
3. Carpenter, L. J. & Liss, P. S. On temperate sources of bromoform and other reactive bromine gases. *J. Geophys. Res.* **105,** 20539–20547 (2002).
4. Hager, L. P., Morris, D. R., Brown, F. S. & Eberwein, H. Chloroperoxidase. II. Utilization of halogen anions. *J. Biol. Chem.* **241,** 1769–1777 (1966).
5. Fenical, W. Halogenation in the Rhodophyta: a review. *J. Phycol.* **11,** 245–259 (1975).
6. Wolinsky, L. E. & Faulkner, D. J. A biomimetic approach to the synthesis of *Laurencia* metabolites. Synthesis of 10-bromo-α-chamigrene. *J. Org. Chem.* **41,** 597–600 (1976).
7. Manthey, J. A. & Hager, L. P. Characterization of the catalytic properties of bromoperoxidase. *Biochemistry* **28,** 3052–3057 (1989).
8. Manthey, J. A. & Hager, L. P. Characterization of the oxidized states of bromoperoxidase. *J. Biol. Chem.* **260,** 9654–9659 (1985).
9. Roach, M. P. *et al. Notomastus lobatus* chloroperoxidase and *Amphitrite ornata* dehaloperoxidase both contain histidine as their proximal heme iron ligand. *Biochemistry* **36,** 2197–2202 (1997).
10. Vilter, H. Peroxidases from Phaeophyceae. III. Catalysis of halogenation by peroxidases from *Ascophyllum nodosum* (L.) Le Jol. *Bot. Mar.* **26,** 429–435 (1983).
11. Vilter, H. Peroxidases from Phaeophyceae. A vanadium(v)-dependent peroxidase from *Ascophyllum nodosum*. *Phytochemistry* **23,** 1387–1390 (1984).
12. Wever, R., Plat, H. & De Boer, E. Isolation procedure and some properties of the bromoperoxidase from the seaweed *Ascophyllum nodosum*. *Biochim. Biophys. Acta* **830,** 181–186 (1985).
13. Vaillancourt, F. H., Yin, J. & Walsh, C. T. SyrB2 in syringomycin E biosynthesis is a nonheme Fe^{II} α-ketoglutarate- and O_2-dependent halogenase. *Proc. Natl Acad. Sci. USA* **102,** 10111–10116 (2005).
14. Chen, X. & van Pée, K.-H. Catalytic mechanisms, basic roles, and biotechnological and environmental significance of halogenating enzymes. *Acta Biochim. Biophys. Sin. (Shanghai)* **40,** 183–193 (2008).
15. Deng, H. & O'Hagan, D. The fluorinase, the chlorinase and the duf-2 enzymes. *Curr. Opin. Chem. Biol.* **12,** 582–592 (2008).
16. Wuosmaa, A. M. & Hager, L. P. Methyl chloride transferase: a carbocation route for biosynthesis of halometabolites. *Science* **249,** 160–162 (1990).
17. Blasiak, L. C. & Drennan, C. L. Structural perspective on enzymatic halogenation. *Acc. Chem. Res.* **42,** 147–155 (2009).
18. Wagner, C., Omari, E. M. & König, G. M. Biohalogenation: nature's way to synthesize halogenated metabolites. *J. Nat. Prod.* **72,** 540–553 (2009).
19. Neumann, C. S., Fujimori, D. G. & Walsh, C. T. Halogenation strategies in natural product biosynthesis. *Chem. Biol.* **15,** 99–109 (2008).
20. Fujimori, D. G. & Walsh, C. T. What's new in enzymatic halogenations. *Curr. Opin. Chem. Biol.* **11,** 553–560 (2007).
21. Littlechild, J., Rodriguez, E. G. & Isupov, M. Vanadium containing bromoperoxidase — insights into the enzymatic mechanism using X-ray crystallography. *J. Inorg. Biochem.* **103,** 617–621 (2009).
22. Vaillancourt, F. H., Yeh, E., Vosburg, D. A., Garneau-Tsodikova, S. & Walsh, C. T. Nature's inventory of halogenation catalysts: oxidative strategies predominate. *Chem. Rev.* **106,** 3364–3378 (2006).
This review summarizes the halogenating enzymes with particular insight into the Fe_{NH}–αKG halogenases.
23. Butler, A. & Carter-Franklin, J. N. A role for vanadium bromoperoxidase in the biosynthesis of halogenated marine natural products. *Nat. Prod. Rep.* **21,** 180–188 (2004).
24. Sundaramoorthy, M., Terner, J. & Poulos, T. L. The crystal structure of chloroperoxidase: a heme peroxidase–cytochrome P450 functional hybrid. *Structure* **3,** 1367–1378 (1995).
25. Kuhnel, K., Blankenfeldt, W., Terner, J. & Schlinchting, I. Crystal structures of chloroperoxidase with its bound substrates and complexed with formate, acetate and nitrate. *J. Biol. Chem.* **281,** 23990–23998 (2006).
26. Wagenknecht, H.-A. & Wolf-Dietrich, W. Identification of intermediates in the catalytic cycle of chloroperoxidase. *Chem. Biol.* **4,** 367–372 (1997).
27. Libby, R. D., Beachy, T. M. & Phipps, A. K. Quantitating direct chlorine transfer from enzyme to substrate in chloroperoxidase-catalyzed reactions. *J. Biol. Chem.* **271,** 21820–21827 (1996).
28. Reddy, C. M. *et al.* A chlorine isotope effect for enzyme-catalyzed chlorination. *J. Am. Chem. Soc.* **124,** 14526–14527 (2002).
This paper established $^{35}Cl/^{37}Cl$ isotope fractionation for the first time in a haloperoxidase during turnover.
29. Van Schijndel, J. W. P. M., Vollenbroek, E. G. M. & Wever, R. The chloroperoxidase from the fungus *Curvularia inaequalis*: a novel vanadium enzyme. *Biochim. Biophys. Acta* **1161,** 249–256 (1993).
30. Winter, J. M. *et al.* Molecular basis for chloronium-mediated meroterpene cyclization. Cloning, sequencing, and heterologous expression of the napyradiomycin biosynthetic gene cluster. *J. Biol. Chem.* **282,** 16362–16368 (2007).
31. Küpper, F. C. *et al.* Iodide accumulation provides kelp with an inorganic antioxidant impacting atmospheric chemistry. *Proc. Natl Acad. Sci. USA* **105,** 6954–6958 (2008).
32. Ortiz-Bermudez, P. *et al.* Chlorination of lignin by ubiquitous fungi has a likely role in global organochlorine production. *Proc. Natl Acad. Sci. USA* **104,** 3895–3900 (2007).
33. Weyand, M. *et al.* X-ray structure determination of a vanadium-dependent haloperoxidase from *Ascophyllum nodosum* at 2.0 Å resolution. *J. Mol. Biol.* **293,** 595–611 (1999).
34. Isupov, M. N. *et al.* Crystal structure of dodecameric vanadium-dependent bromoperoxidase from the red algae *Corallina officinalis*. *J. Mol. Biol.* **299,** 1035–1049 (2000).
35. Messerschmidt, A. & Wever, R. X-ray structure of a vanadium containing enzyme: chloroperoxidase from the fungus *Curvularia inaequalis*. *Proc. Natl Acad. Sci. USA* **93,** 392–396 (1996).
36. Colpas, G. J., Hamstra, B. J., Kampf, J. W. & Pecoraro, V. L. Functional models for vanadium haloperoxidases: reactivity and mechanism of halide oxidation. *J. Am. Chem. Soc.* **118,** 3469–3478 (1996).
37. Hemrika, W., Rokus, R., Macedo-Ribeiro, S., Messerschmidt, A. & Wever, R. Heterologous expression of the vanadium-containing chloroperoxidases from *Curvularia inaequalis* in *Saccharomyces cerevisiae* and site-directed mutagenesis of the active site residues His^{496}, Lys^{353}, Arg^{360}, and Arg^{490}. *J. Biol. Chem.* **274,** 23820–23827 (1999).
38. Everett, R. R., Kanofsky, J. R. & Butler, A. Mechanism of dioxygen formation catalyzed by vanadium bromoperoxidase. Steady state kinetic analysis and comparison to the mechanism of bromination. *J. Biol. Chem.* **265,** 15671–15679 (1990).
39. Tschirret-Guth, R. A. & Butler, A. Evidence for organic substrate binding to vanadium bromoperoxidase. *J. Am. Chem. Soc.* **116,** 411–412 (1994).
40. Carter-Franklin, J. N., Parrish, J. D., Tschirret-Guth, R. A., Little, R. D. & Butler, A. Vanadium haloperoxidase-catalyzed bromination and cyclization of terpenes. *J. Am. Chem. Soc.* **125,** 3688–3689 (2003).
41. Carter-Franklin, J. N. & Butler, A. Vanadium bromoperoxidase-catalyzed biosynthesis of halogenated marine natural products. *J. Am. Chem. Soc.* **126,** 15060–15066 (2004).
This paper shows diasteroselectivity of a V-BPO-catalysed reaction for the first time in the bromination and cyclization of the terpene (*E*)-(+)-nerolidol.
42. Wang, Y. J., Huang, J. J. & Leadbetter, J. R. Acyl-HSL signal decay: intrinsic to bacterial cell-cell communications. *Adv. Appl. Microbiol.* **61,** 27–58 (2007).
43. Steinberg, P. D., de Nys, R. & Kjelleberg, S. in *Marine Chemical Ecology* (eds McClintock, J. B. & Baker, B. J.) 355–387 (CRC, 2001).
44. Borchardt, S. A. *et al.* Reaction of acylated homoserine lactone bacterial signaling molecules with oxidized halogen antimicrobials. *Appl. Environ. Microbiol.* **67,** 3174–3179 (2001).
45. Blasiak, L. C., Vaillancourt, F. H., Walsh, C. T. & Drennan, C. L. Crystal structure of the non-haem iron halogenase SyrB2 in syringomycin biosynthesis. *Nature* **440,** 368–371 (2006).
46. Hanauske-Abel, H. M. & Popowicz, A. M. The HAG mechanism: a molecular rationale for the therapeutic application of iron chelators in human diseases involving the 2-oxoacid utilizing dioxygenases. *Curr. Med. Chem.* **10,** 1005–1019 (2003).
47. Matthews, M. L. *et al.* Substrate-triggered formation and remarkable stability of the C–H bond-cleaving chloroferryl intermediate in the aliphatic halogenase, SyrB2. *Biochemistry* **48,** 4331–4343 (2009).
This paper provides significant mechanistic insight into the reactions catalysed by the Fe_{NH}–αKG halogenases in comparison with those catalysed by the Fe_{NH}–αKG oxygenases.
48. Galonic, D. P., Vaillancourt, F. H. & Walsh, C. T. Halogenation of unactivated carbon centers in natural product biosynthesis: trichlorination of leucine during barbamide biosynthesis. *J. Am. Chem. Soc.* **128,** 3900 (2006).
49. Chang, Z. *et al.* The barbamide biosynthetic gene cluster: a novel marine cyanobacterial system of mixed polyketide synthase (PKS)-non ribosomal peptide synthetase (NRPS) origin involving an unusual trichloroleucyl starter unit. *Gene* **296,** 235–247 (2002).
50. Ueki, M. *et al.* Enzymatic generation of the antimetabolite γ, γ-dichloroaminobutyrate by NRPS and mononuclear iron halogenase action in a streptomycete. *Chem. Biol.* **13,** 1183–1191 (2006).
51. Vaillancourt, F. H., Yeh, E., Vosburg, D. A., O'Connor, S. E. & Walsh, C. T. Cryptic chlorination by a non-haem iron enzyme during cyclopropyl amino acid biosynthesis. *Nature* **436,** 1191–1194 (2005).
This paper is the first report of cyclopropyl formation via a chlorinated precursor.
52. Chang, Z. *et al.* Biosynthetic pathway and gene cluster analysis of curacin A, an antitubulin natural product from the tropical marine cyanobacterium *Lyngbya majuscula*. *J. Nat. Prod.* **67,** 1356–1367 (2004).
53. Edwards, D. J. *et al.* Structure and biosynthesis of the jamaicamides, new mixed polyketide-peptide neurotoxins from the marine cyanobacterium *Lyngbya majuscula*. *Chem. Biol.* **11,** 817–833 (2004).
54. Gu, L. *et al.* Metamorphic enzyme assembly in polyketide diversification. *Nature* **459,** 731–735 (2009).
This paper demonstrates coevolution of enzymes for metabolic diversification in the biosynthetic pathways leading to β-branched cyclopropane in curacin A and a vinyl chloride in jamaicamide A.
55. Ni, X. & Hager, L. P. cDNA cloning of *Batis maritima* methyl chloride transferase and purification of the enzyme. *Proc. Natl Acad. Sci. USA* **95,** 12866–12871 (1998).
56. Eustaquio, A. S., Pojer, F., Noe, J. P. & Moore, B. S. Discovery and characterization of a marine bacterial SAM-dependent chlorinase. *Nature Chem. Biol.* **4,** 69–74 (2008).
57. Dong, C. *et al.* Crystal structure and mechanism of a bacterial fluorinating enzyme. *Nature* **427,** 561–565 (2004).
58. Deng, H. *et al.* The fluorinase from *Streptomyces cattleya* is also a chlorinase. *Angew. Chem. Int. Ed.* **45,** 759–762 (2006).
5 9. Cadicamo, C. D., Courtieu, J., Deng, H., Meddour, A. & O'Hagan, D. Enzymatic fluorination in *Streptomyces cattleya* takes place with an inversion of configuration consistent with an SN2 reaction mechanism. *ChemBioChem* **5,** 685–690 (2004).
60. Michels, J. J., Allain, E. J., Borchardt, S. A., Hu, P. & McCoy, W. F. Degradation pathway of homoserine lactone bacterial signal molecules by halogen antimicrobials identified by liquid chromatography with photodiode array and mass spectrometric detection. *J. Chromatogr. A* **898,** 153–165 (2000).

Acknowledgements A.B. greatly acknowledges US National Science Foundation Division of Chemistry award number 0719553 for support of her research.

Author Information Reprints and permissions information is available at www.nature.com/reprints. The authors declare no competing financial interests. Correspondence should be addressed to A.B. (butler@chem.ucsb.edu).